



Cite this: DOI: 10.1039/c5cc00934k

Received 1st February 2015,
Accepted 17th March 2015

DOI: 10.1039/c5cc00934k

www.rsc.org/chemcomm

Fluorescence responsive conjugated poly(tetraphenylethene) and its morphological transition from micelle to vesicle†

Lipeng He, Xiaoning Liu, Jianjun Liang, Yong Cong, Zhenyu Weng and Weifeng Bu*

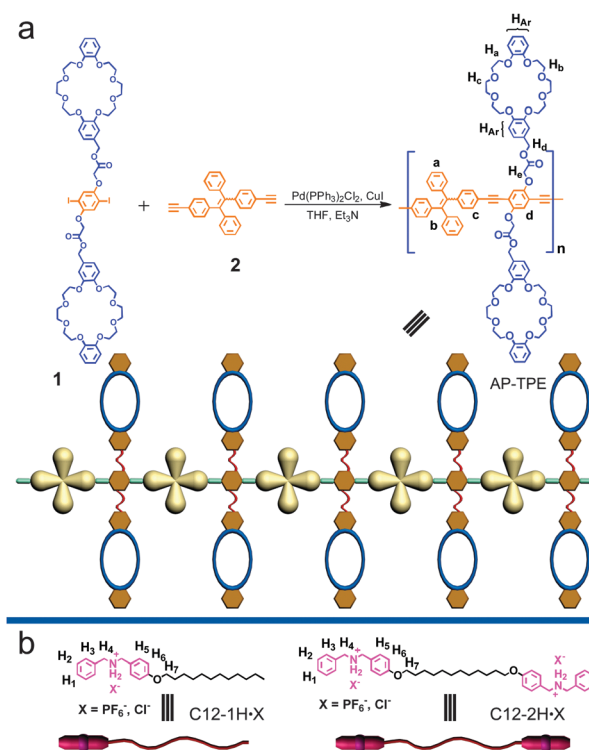
A crown ether-functionalized poly(tetraphenylethene) (AP-TPE) is synthesized and the rotation of the TPE group is successfully restricted via the complexation of crown ether and organic ammonium salts, leading to a stepwise enhanced fluorescence accompanied by a morphological transition from micellar to vesicular.

Owing to high quantum yield, excellent photophysical stability and facile surface modification, conjugated polymers (CPs) have drawn wide attention in the fields of optoelectronics and biology in recent years.¹ However, the conventional CPs often show weak or quenched fluorescence in their concentrated solutions and aggregate states because of the aggregation-caused quenching effect, which has limited their real applications in devices such as light-emitting diodes (LEDs) and bio-imaging/sensors.^{2,3} Recently, aggregation-induced emission (AIE) and aggregation-induced emission enhancement (AIEE) have been demonstrated as promising methods to tackle the defect.⁴ In the AIE/AIEE systems, luminogens are non-emissive or weakly emissive in the dilute solution but significantly emissive in their concentrated solutions and/or aggregated states. Therefore, incorporation of AIE luminogens (AIEgens) into CPs is a significant attempt to avoid fluorescence quenching.³ In AIEgen-containing CPs, the steric effect of the rigid chain suppresses intra-molecular motions of AIEgens and thus their emission is remarkably enhanced.³

On the other hand, supramolecular polymers (SPs) have also emerged in the optoelectronic and biological fields due to their multiple responsiveness, superb self-healing and degradability.⁵ Combining non-covalent interactions with conjugated molecules, we⁶ and others⁷ have developed various fluorescence responsive SPs, many of which exhibit fluorescence quenching or weakening upon non-covalent interactions. We therefore ask whether such studies

can be extended to the AIE and AIEE systems. To date, several non-covalent interactions have been used to activate the AIE/AIEE feature successfully.⁸ However, these systems do not show significant fluorescence responsiveness to external stimuli. In this communication, we have synthesized an AIEgen-containing conjugated polymer (AP-TPE) (Scheme 1). Upon treatment of the solution of AP-TPE successively with acid and base, the fluorescence intensity was remarkably enhanced and decreased, respectively, together with a morphological transition from micellar to vesicular aggregates.

AP-TPE was synthesized *via* the Sonogashira cross-coupling reaction of dibenzo-24-crown-8 (DB24C8)-substituted 1,4-diiodobenzene



Scheme 1 (a) Synthetic approach of AP-TPE; (b) chemical structures of the guest molecules, C12-1H-X and C12-2H-X, X = Cl and PF₆.

Key Laboratory of Nonferrous Metals Chemistry and Resources Utilization of Gansu Province, State Key Laboratory of Applied Organic Chemistry and College of Chemistry and Chemical Engineering, Lanzhou University, Lanzhou, Gansu, China. E-mail: buwf@lzu.edu.cn

† Electronic supplementary information (ESI) available: Experimental procedures and full characterizations of AP-TPE, C12-1, C12-1H-PF₆, C12-2 and C12-2H-PF₆, additional DLS plots and TEM images. See DOI: 10.1039/c5cc00934k

(1) and 1,2-bis(4-ethynylphenyl)-1,2-diphenylethene (2) as shown in Scheme 1a. ^1H NMR (Fig. S4 and S5, ESI †), gel permeation chromatography methods (Fig. S6, ESI †) and infrared spectra (Fig. S7, ESI †) confirmed the successful polymerization reaction and the formation of AP-TPE. UV-vis absorption spectra of 2 and AP-TPE in their THF solutions (10 μM) are depicted in Fig. S20 (ESI †). In comparison with 2, the absorption band of AP-TPE showed a large red-shift from 329 to 378 nm, agreeing well with the high conjugation of AP-TPE.^{1b,3b} Upon excitation at 375 nm, AP-TPE in pure THF exhibited a weak fluorescence, which was similar with the reported TPE-based polymer.³ Considering the AIE feature of AP-TPE, an amount of water was added to the THF solution of AP-TPE. As shown in Fig. 1, with the increase of water fraction, the fluorescence intensity of AP-TPE started to increase and reached its maximum value at 70% water content, which was 4.6 times higher than that in pure THF solution. However, when the water content increased to 90%, the fluorescence intensity dropped to some extent. This was because the precipitation of the large-sized aggregates decreased the effective AP-TPE concentration in the solution.⁹ Besides this, amorphous aggregates abruptly formed at 90% water content could trap the solvent molecules inside. In these loose aggregates, the intramolecular motions of TPE groups were not restricted completely, which also decreased the emission.⁹ From the inner photographs in Fig. 1b, we could catch sight of the weak emission in THF solution but strong emission in the mixed solvent of 90% water content.

The complexation between AP-TPE and guest groups was initially investigated by ^1H NMR spectroscopy as shown in Fig. S22 (ESI †) and Fig. 2. Upon treatment of AP-TPE (0.5 mM) with 1.0 equivalent of C12-2H-PF₆, the resonance signals of DB24C8 moieties and dibenzylammonium salts (DBAs) shifted significantly and became more broadened (Fig. 2a and b). Among these signals, the benzyl protons H₄ of C12-2H-PF₆ shifted downfield from $\delta = 4.15$ to 4.50 ppm, while the others shifted upfield. No uncomplexed signal was detected, indicating that the crown ether moieties were completely threaded by the DBA groups and thus the network complex was formed as shown in Fig. S21 (ESI †). Subsequent *in situ* addition of 2.0 equivalents of *N*-*tert*-butyl-*N'*,*N'*,*N''*,*N''*,*N'''*,*N'''*-hexamethylphosphorimidic triamide (P₁-*t*Bu) caused the deprotonation of C12-2H-PF₆ and the complexed resonance consequently disappeared. The resulting ^1H NMR spectrum originated from the combined signals of AP-TPE and neutral C12-2 (Fig. 2c). And then,

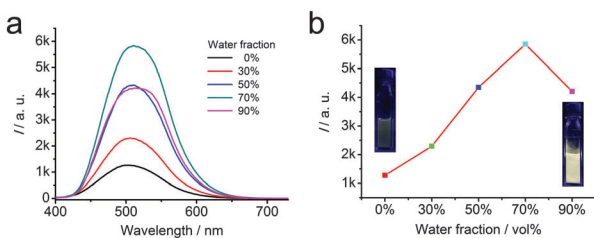


Fig. 1 (a) Fluorescence spectra excited at 375 nm and (b) the plot of fluorescence intensity of AP-TPE (10 μM) in THF–water mixture solvents with different water fractions. The inner photographs show AP-TPE in the mixed THF–water solvent at 0% and 90% water content under UV irradiation. The concentration referred to the monomer concentration.

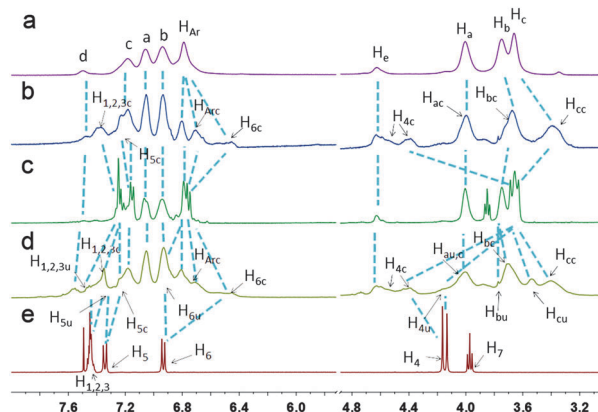


Fig. 2 Partial ^1H NMR spectra (400 MHz, CD_2Cl_2) of (a) 0.5 mM AP-TPE, (b) 0.5 mM AP-TPE (monomer concentration) and 1.0 equivalent of C12-2 H-PF₆ (DBA/DB24C8 1:1 molar ratio), (c) obtained by adding 2.0 equivalents of P₁-*t*Bu to (b), (d) obtained by adding 2.0 equivalents of CF₃COOH to (c), and (e) guest C12-2H-PF₆ ($\text{CDCl}_3/\text{CD}_3\text{CN}$, 1/1). Here “u” and “c” denote uncomplexed and complexed moieties, respectively.

2.0 equivalents of CF₃COOH were successively added, leading to the appearance of the complexed ^1H NMR signals again, but together with small amounts of uncomplexed DB24C8 and DBA resonances (Fig. 2d), which were slightly different from those shown in Fig. 2b. Similarly, the addition of C12-1H-PF₆ to AP-TPE also gave rise to comparable ^1H NMR spectral changes as described above (Fig. S22, ESI †).

Next, we examined the sizes of the above-mentioned host–guest complexes through dynamic light scattering (DLS) and transmission electron microscopy (TEM) measurements. The results of DLS experiments are shown in Fig. S23a (ESI †) and Fig. 3a. In the DLS plot, AP-TPE exhibited a narrow band centred at a hydrodynamic diameter (D_h) of 185 nm, which was much larger than the length of the polymer (*ca.* 39 nm based on DP = 20), probably due to aggregation of AP-TPE under the present solvent condition. After the complexation with C12-2H-PF₆, the D_h of the network complexes increased to 294 nm together with a much broader signal. Correspondingly, TEM images revealed that irregular aggregates (Fig. S24, ESI †) evolved to spherical nanostructures with diameters of 250–400 nm (Fig. 3b and c). Upon addition of 2.0 equivalents of P₁-*t*Bu to the complexes, D_h returned back to the original location. However, almost no change in D_h s was detected during the self-assembly of AP-TPE and C12-1H-PF₆ (Fig. S23a, ESI †).

Interestingly, we therefore asked whether the aggregation could activate the AIEE nature of AP-TPE. Upon addition of C12-2H-PF₆, the fluorescence band of AP-TPE (0.5 mM) centred at 525 nm showed a clear increase in intensity (Fig. 3d), which agreed well with the increase in D_h as described above. Instead of treatment with extra host and/or guest molecules as demonstrated in previous pillar arene-based AIEE systems,⁸ the facile addition of P₁-*t*Bu completely restored the enhanced emission to the original level. The difference was that only less fluorescence enhancement was observed in the case of C12-1H-PF₆ and AP-TPE, consistent with the slight increase in D_h (Fig. S23, ESI †). Corresponding to previous experimental studies,^{4,6d} the host–guest recognition restricts the intramolecular rotation of TPE moieties or other AIEgens at the

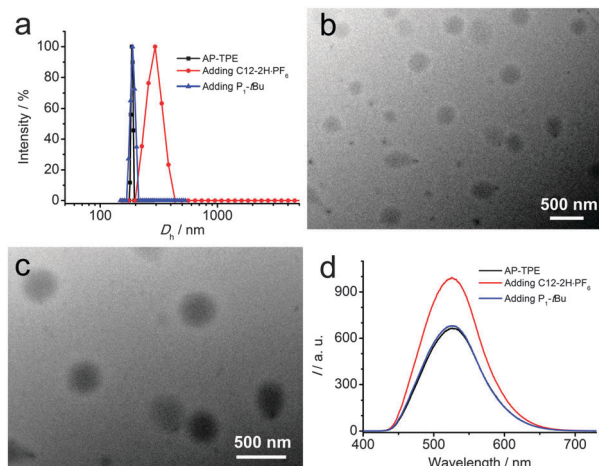


Fig. 3 (a) DLS plot of AP-TPE, (b and c) TEM images of aggregates of AP-TPE and (d) fluorescence responsiveness of AP-TPE upon successive treatment with C12-2H-PF₆ and P₁-tBu (CH₂Cl₂, 0.5 mM).

molecular level and the non-radiative pathway is blocked, leading to a visible fluorescence enhancement. Comparatively, in the case of the network complex formed by C12-2H-PF₆ and AP-TPE, both the intra- and intermolecular rotations were restricted due to the cross-linked topological structure and thus the fluorescence was significantly enhanced. When the base was added, the intra- and intermolecular motions were not suppressed any more and the fluorescence was thus recovered. These facts highlighted the fact that the aggregation benefiting from the host-guest interaction of DB24C8 and DBA groups can activate the AIEE feature to a great extent in the present case.

However, the present fluorescence enhancement was rather less than that of TPE-based CPs in the mixed THF-water solvents (Fig. 1).³ In contrast with the threading structure of DB24C8 with DBA-PF₆,^{10a-d} DB24C8 can bind DBA with the chloride counter anion *via* the N-H...O hydrogen bond in a face-to-face manner, and form a more compact and ordered matrix.^{10e,f} Upon successive treatment of HCl and NaOH, we therefore monitored fluorescence changes of the THF solution containing AP-TPE and C12-1/C12-2. The experimental data are depicted in Fig. S25 (ESI[†]) and Fig. 4. When 2.0 equivalents of HCl were added to the neutral solution of AP-TPE/C12-2, the solution became turbid immediately (Fig. S26, ESI[†]). Meanwhile, the fluorescence spectra revealed an amazing

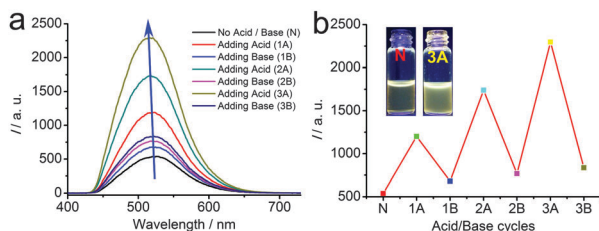


Fig. 4 (a) Fluorescence spectra and (b) the plot of fluorescence intensity of AP-TPE/C12-2 in THF treated with HCl and NaOH, repeatedly. The concentrations of AP-TPE and C12-2 were 0.5 mM. The concentrations of HCl and NaOH were 1.0 M in H₂O. Here, N, A and B denote the neutral solution and its acid and base treatments, respectively. 1, 2 and 3 denote the sequence of the acid-base cycle.

fact that there was a 2.2 times increase in the fluorescence intensity (Fig. 4a and b). Subsequent addition of 2.0 equivalents of NaOH led to a transparent solution accompanied by a decrease in fluorescence. Afterwards, the solution was treated with the acid-base cycles twice and the fluorescence became stronger step by step (Fig. 4a and b). The fluorescence intensity increased nearly 4.3 times after the third acidification. Furthermore, we carried out several control experiments to explain the phenomenon (Fig. S27, ESI[†]) and found that the interaction between DB24C8 and DBA and the salting-out effect played leading roles in such a stepwise enhanced fluorescence. According to the previous studies,¹¹ when the TPE moiety took a tighter packing in crystals or highly ordered structures, the intra-molecular motion was restricted more completely, thus leading to stronger and blue-shifted emissions. In our system, the blue-shift of the emission peak from 523 to 514 nm had certified a more and more compact packing of AP-TPE molecules. No significant change was detected in the fluorescence intensity when the THF solution of AP-TPE and C12-1 was treated with the same acid-base cycles (Fig. S25, ESI[†]).

To understand the observed phenomena, DLS and TEM measurements were employed to check the D_h s and aggregate structures of the complexes. In the initial solution of AP-TPE and C12-2, the DLS plot exhibited a narrow band centred at 338 nm (Fig. 5a). Upon acid treatment with HCl, the complexation of DB24C8 and DBA moieties occurred, leading to the formation of supramolecular assemblies. Consequently, the value of D_h increased to 492 nm and spherical micelles were observed in TEM images (Fig. 5b). The ordered micellar aggregates resulted in a much stronger fluorescence as shown in Fig. 4. When the solution was subsequently treated with NaOH, the fluorescence intensity dropped remarkably. However, the DLS plot extraordinarily displayed that D_h of the mixture did not revert back to its original value but increased to 631 nm with a broad distribution (Fig. 5a). We therefore speculated that AP-TPE might form some large but unordered aggregates in the solution after the first acid-base cycle. As expected, irregular and unordered aggregates were clearly observed in TEM images (Fig. S30, ESI[†]), substantiating our speculation. In the latter two cycles, the DLS plots exhibited a similar trend and the only difference from the first cycle was that the sizes of aggregates grew stepwise to 586 and 622 nm upon acidification, respectively.

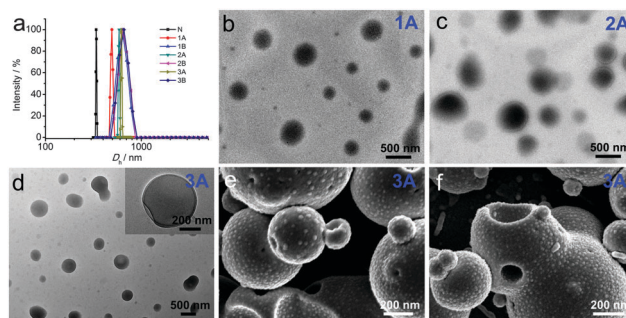


Fig. 5 (a) DLS plot of AP-TPE and C12-2 in THF treated with HCl and NaOH repeatedly. (b-d) TEM images of AP-TPE and C12-2 after the first, second and third acidification. (e and f) SEM images of AP-TPE and C12-2 after the third acidification.

As shown in Fig. 5c, the self-assembly of AP-TPE with C12-2 formed spherical aggregates with diameters of 400–600 nm after the second acidification. The spherical aggregates showed a clear contrast between the exterior and interior, which was consistent with the typical feature of vesicles. After the third acidification, many more legible vesicles were observed with diameters ranging from ca. 500 to 700 nm (Fig. 5d). To confirm the vesicular structure, scanning electron microscopy (SEM) measurement was further performed (Fig. 5e and f). Several collapsed and ruptured vesicles were captured. Furthermore, the inside and outside of ruptured vesicles were clearly observed. Usually, vesicular aggregates originated from the solvophobic self-assembly of molecules in a specific solvent.¹² In our case, DB24C8 bound with DBA to form polar groups after the first acidification. As a result of the solvophobic effect, the complex formed the micelle and the polar groups were located on the inner side of the micelle. The subsequent acid–base reaction led to the generation of NaCl, which further promoted the aggregation due to the salting-out effect. Until the next acidification, both the interaction between DB24C8 and DBA and the salting-out effect modified the solvophilic–solvophobic effect and the system reached a new balance, and thus a highly ordered vesicle was formed. These changes were consistent with the step-wise enhanced fluorescence and blue-shifted emission peaks.¹¹ To the best of our knowledge, such a morphological transition-induced step-by-step enhancement has seldom been brought out in the previous AIE/AIEE systems.^{3,4,8,11}

In summary, we have confirmed in our attempt that the complexation of DB24C8 and DBA groups can suppress the motion of the TPE moiety and thus activate the AIEE feature of AP-TPE. Particularly, the reduplicative complexation of AP-TPE and C12-2H-Cl not only enhances the fluorescence remarkably, but also induces a morphological transformation from micellar to vesicular. Moreover, it is emphasized that such acid–base responsive vesicular assembly/disassembly has a potential for encapsulation and release of small molecules such as drugs and dyes.

This work was supported by the NSFC (51173073 and J1103307), the Fundamental Research Funds for the Central Universities (lzujbky-2014-74) and the Open Project of State Key Laboratory of Supramolecular Structure and Materials of Jilin University (sklssm201502).

Notes and references

- (a) S. W. Thomas, G. D. Joly and T. M. Swager, *Chem. Rev.*, 2007, **107**, 1339; (b) T. L. Andrew and T. M. Swager, *J. Polym. Sci., Part B: Polym. Phys.*, 2011, **49**, 476; (c) B. Liu and G. C. Bazan, *Conjugated Polyelectrolytes: Fundamentals and Applications*, Wiley, 2013; (d) K. Müllen, J. R. Reynolds and T. Masuda, *Conjugated Polymers: A Practical Guide to Synthesis*, RSC, 2014.
- (a) S. A. Jenekhe and J. A. Osaheni, *Science*, 1994, **265**, 765; (b) B. Valeur, M. N. Berberan-Santos, *Molecular Fluorescence: Principles and Applications*, Wiley-VCH Verlag & Co., Weinheim, Germany, 2nd edn, 2013.
- (a) R. Hu, N. L. C. Leung and B. Z. Tang, *Chem. Soc. Rev.*, 2011, **40**, 5361; (b) R. Hu, J. L. Maldonado, M. Rodriguez, C. Deng, C. K. W. Jim, J. W. Y. Lam, M. M. F. Yuen, G. Ramos-Ortiz and B. Z. Tang, *J. Mater. Chem.*, 2012, **22**, 232.
- (a) J. Luo, Z. Xie, J. W. Y. Lam, L. Cheng, H. Chen, C. Qiu, H. S. Kwok, X. Zhan, Y. Liu, D. Zhu and B. Z. Tang, *Chem. Commun.*, 2001, 1740; (b) B.-K. An, S.-K. Kwon, S.-D. Jung and S. Y. Park, *J. Am. Chem. Soc.*, 2002, **124**, 14410; (c) L. Liu, G. Zhang, J. Xiang, D. Zhang and D. Zhu, *Org. Lett.*, 2008, **10**, 4581; (d) J. He, B. Xu, F. Chen, H. Xia, K. Li, L. Ye and W. Tian, *J. Phys. Chem. C*, 2009, **113**, 9892; (e) Q. Chen, N. Bian, C. Cao, X.-L. Qiu, A.-D. Qi and B.-H. Han, *Chem. Commun.*, 2010, **46**, 4067; (f) H. Lu, B. Xu, Y. Dong, F. Chen, Y. Li, Z. Li, J. He, H. Li and W. Tian, *Langmuir*, 2010, **26**, 6838; (g) X. Wang, J. Hu, T. Liu, G. Zhang and S. Liu, *J. Mater. Chem.*, 2012, **22**, 8622; (h) Z. Wang, S. Chen, J. W. Y. Lam, W. Qin, R. T. K. Kwok, N. Xie, Q. Hu and B. Z. Tang, *J. Am. Chem. Soc.*, 2013, **135**, 8238; (i) Z. Wang, B. Xu, L. Zhang, J. Zhang, T. Ma, J. Zhang, X. Fu and W. Tian, *Nanoscale*, 2013, **5**, 2065; (j) R. Yoshii, A. Hirose, K. Tanaka and Y. Chujo, *J. Am. Chem. Soc.*, 2014, **136**, 18131.
- (a) P. Cordier, F. Tournilhac, C. Soulie-Ziakovic and L. Leibler, *Nature*, 2008, **451**, 977; (b) M. Burnworth, L. Tang, J. R. Kumpfer, A. J. Duncan, F. L. Beyer, G. L. Fiore, S. J. Rowan and C. Z. Weder, *Nature*, 2011, **472**, 334; (c) S. Seiffert and J. Sprakel, *Chem. Soc. Rev.*, 2012, **41**, 909; (d) S.-L. Li, T. Xiao, C. Lin and L. Wang, *Chem. Soc. Rev.*, 2012, **41**, 5950; (e) T. Aida, E. W. Meijer and S. I. Stupp, *Science*, 2012, **335**, 813; (f) B. C. Tee, C. Wang, R. Allen and Z. Bao, *Nat. Nanotechnol.*, 2012, **7**, 825; (g) Z. Huang, L. Yang, Y. Liu, Z. Wang, O. A. Scherman and X. Zhang, *Angew. Chem., Int. Ed.*, 2014, **53**, 5351; (h) P. Wei, X. Yan and F. Huang, *Chem. Soc. Rev.*, 2015, **44**, 815.
- (a) B. Yu, B. Wang, S. Guo, Q. Zhang, X. Zheng, H. Lei, W. Liu, W. Bu, Y. Zhang and X. Chen, *Chem. – Eur. J.*, 2013, **19**, 4922; (b) B. Yu, S. Guo, L. He and W. Bu, *Chem. Commun.*, 2013, **49**, 3333; (c) S. Guo, J. Zhang, B. Wang, Y. Cong, X. Chen and W. Bu, *RSC Adv.*, 2014, **4**, 51754; (d) L. He, J. Liang, Y. Cong, X. Chen and W. Bu, *Chem. Commun.*, 2014, **50**, 10841.
- X. Ji, Y. Yao, J. Li, X. Yan and F. Huang, *J. Am. Chem. Soc.*, 2013, **135**, 74.
- (a) P. Wang, X. Yan and F. Huang, *Chem. Commun.*, 2014, **50**, 5017; (b) J. Wu, S. Sun, X. Feng, J. Shi, X.-Y. Hu and L. Wang, *Chem. Commun.*, 2014, **50**, 9122; (c) N. Song, D.-X. Chen, M.-C. Xia, X.-L. Qiu, K. Ma, B. Xu, W. Tian and Y.-W. Yang, *Chem. Commun.*, 2015, **51**, 5526.
- (a) Y. Hong, S. Chen, C. W. T. Leung, J. W. Y. Lam, J. Liu, N.-W. Tseng, R. T. K. Kwok, Y. Yu, Z. Wang and B. Z. Tang, *ACS Appl. Mater. Interfaces*, 2011, **3**, 3411; (b) E. Wang, J. W. Y. Lam, R. Hu, C. Zhang, Y. S. Zhao and B. Z. Tang, *J. Mater. Chem. C*, 2014, **2**, 1801; (c) J. Huang, Y. Jiang, J. Yang, R. Tang, N. Xie, Q. Li, H. S. Kwok, B. Z. Tang and Z. Li, *J. Mater. Chem. C*, 2014, **2**, 2028.
- (a) P. R. Ashton, P. J. Campbell, E. J. T. Chrystal, P. T. Glink, S. Menzer, D. Philp, N. Spencer, J. F. Stoddart, P. A. Tasker and D. J. Williams, *Angew. Chem., Int. Ed. Engl.*, 1995, **34**, 1865; (b) A. G. Kolchinski, D. H. Busch and N. W. Alcock, *J. Chem. Soc., Chem. Commun.*, 1995, 1289; (c) M. Han, H.-Y. Zhang, L.-X. Yang, Q. Jiang and Y. Liu, *Org. Lett.*, 2008, **10**, 5557; (d) H.-B. Cheng, H.-Y. Zhang and Y. Liu, *J. Am. Chem. Soc.*, 2013, **135**, 10190; (e) S. Dong, B. Zhang, D. Xu, X. Yan, M. Zhang and F. Huang, *Adv. Mater.*, 2012, **24**, 3191; (f) L. Gao, D. Xu and B. Zheng, *Chem. Commun.*, 2014, **50**, 12142.
- (a) X. Wang, J. Hu, T. Liu, G. Zhang and S. Liu, *J. Mater. Chem.*, 2012, **22**, 8622; (b) Z. Zhao, J. W. Y. Lam and B. Z. Tang, *J. Mater. Chem.*, 2012, **22**, 23726; (c) J. Ma, T. Lin, X. Pan and W. Wang, *Chem. Mater.*, 2014, **26**, 4221; (d) W. Bai, Z. Wang, J. Tong, J. Mei, A. Qin, J. Z. Sun and B. Z. Tang, *Chem. Commun.*, 2015, **51**, 1089.
- (a) W. Bu, S. Uchida and N. Mizuno, *Angew. Chem., Int. Ed.*, 2009, **48**, 8281; (b) L. He, S. Bi, H. Wang, B. Ma, W. Liu and W. Bu, *Langmuir*, 2012, **28**, 14164; (c) Q. Zhang, L. He, H. Wang, C. Zhang, W. Liu and W. Bu, *Chem. Commun.*, 2012, **48**, 7067; (d) P. Yin, T. Li, R. S. Forgan, C. Lydon, X. Zuo, Z. N. Zheng, B. Lee, D. Long, L. Cronin and T. Liu, *J. Am. Chem. Soc.*, 2013, **135**, 13425.